

Dipalmitoylation of a cellular uptake-mediating apolipoprotein E-derived peptide as a promising modification for stable anchorage in liposomal drug carriers

Ines Sauer, Heike Nikolenko, Sandro Keller, Khalid Abu Ajaj, Michael Bienert, Margitta Dathe *

Leibniz Institute of Molecular Pharmacology (FMP), Robert-Rössle-Strasse 10, 13125 Berlin, Germany

Received 18 January 2006; received in revised form 6 March 2006; accepted 9 March 2006

Available online 7 April 2006

Abstract

Liposomes equipped with cellular uptake-mediating peptidic vector compounds have attracted much attention as target-specific drug delivery systems. Aside from the development of the target recognition motif itself, vector coupling to liposomes while conserving the active conformation constitutes an important element in carrier development. To elucidate the most efficient way for adsorptive peptide binding to liposomes, we synthesized and characterized two-domain peptides comprising a cationic sequence derived from the binding domain of apolipoprotein E (apoE) for the low-density lipoprotein receptor and different lipid-binding motifs, that is, an amphipathic helix, a transmembrane helix, single fatty acids or two palmitoyl chains. Peptide properties considered relevant for peptide–liposome complexes to initiate an endocytotic cellular uptake such as lipid binding, helicity, stability of anchorage, bilayer-disturbing activity, and toxicity showed that the dipalmitoyl derivative was the most suitable to associate the apoE peptide to the surface of liposomes. The peptide showed pronounced lipid affinity and was stably anchored within the lipid bilayer on a time scale of at least 30 min. The helicity of about 40% in the lipid-bound state and the location of the amphipathic helix on the liposomal surface provided the prerequisites for interaction of the complex with the cell surface-located receptor. The concentration of the dipalmitoylated peptide to permeabilize neutral lipid bilayers (lipid concentration 25 μM) was 0.06 μM and a 2 μM concentration reduced cell viability to about 80%. Efficient internalization of liposomes bearing about 180 peptide derivatives on the surface into brain capillary endothelial cells was monitored by confocal laser scanning microscopy. The concept of complexation using dipalmitoylated peptides may offer an efficient substitute to covalent vector coupling and a prospective way to optimize the capacity of liposomes as drug delivery systems also for different targets.

© 2006 Elsevier B.V. All rights reserved.

Keywords: Lipid-binding domain; Apolipoprotein E; Peptide–liposome complex; Cellular uptake

Abbreviations: ApoE, apolipoprotein E; BBB, blood–brain barrier; CD, circular dichroism; CLSM, confocal laser scanning microscopy; DiBr-PPSPC, 1-palmitoyl-2-stearoyl-(6-7)dibromo-*sn*-glycero-3-phosphocholine; Dde, 1-(4,4-dimethyl-2,6-dioxocyclohex-1-ylidene)ethyl; DMF, dimethyl formamide; DMSO, dimethyl sulfoxide; 5-DOX, 1-palmitoyl-2-stearoyl-(5-DOXYL)-*sn*-glycero-3-phosphocholine; EDTA, ethylenediaminetetraacetic acid; FITC, fluorescein isothiocyanate; Fmoc, 9-fluorenylmethoxycarbonyl; ITC, isothermal titration calorimetry; LUV, large unilamellar vesicle; LDL, low-density lipoprotein; MALDI-TOF, matrix-assisted laser desorption/ionization time-of-flight; MTT, (3-(4,5-dimethylthiazol-2-yl)-2,5-diphenyl)tetrazolium bromide; PBS, phosphate-buffered saline; POPC, 1-palmitoyl-2-oleoyl-*sn*-glycero-3-phosphocholine; Rh-DPPE, 1,2-dipalmitoyl-*sn*-glycero-3-phosphoethanolamine-*N*-[lissamine rhodamine B sulfonyle]; RP-HPLC, reversed-phase high-performance liquid chromatography; SUV, small unilamellar vesicle; TEMPO, 1,2-dioleoyl-*sn*-glycero-3-phospho(TEMPO)choline; Tris, tris(hydroxymethyl)aminomethane; TFA, trifluoroacetic acid; TFE, trifluoroethanol

* Corresponding author. Tel.: +49 30 94793274; fax: +49 30 94793159.

E-mail address: dathe@fmp-berlin.de (M. Dathe).

1. Introduction

Liposomes are advantageous carriers for many drugs as they can be loaded with hydrophobic as well as hydrophilic compounds to overcome unfavorable properties such as poor solubility, low stability, rapid metabolism and toxicity [1,2]. However, in many cases, a lack of specificity still limits the potential advantages of liposomal drug administration. One approach to tackle this problem is carrier derivatization with a ligand that recognizes membrane constituents [3] and mediates drug transport across barriers such as the blood–brain barrier (BBB) [4].

The accessibility of drugs to the central nervous system is highly limited by the blood–brain barrier. The continuous layer of

endothelial cells connected by tight junctions prevents paracellular permeation [5]. A promising strategy to overcome this barrier is the activation of transcytotic transport routes [6]. So far, evidence for vector-mediated drug delivery to the brain is most convincing for immunoliposomes equipped with monoclonal antibodies against the transferrin receptor [7,8].

The BBB is also rich in the low-density lipoprotein receptor (LDLR) [9]. Its role in the transcytotic uptake of cholesterol-rich lipoproteins into the brain has been demonstrated [10]. One ligand for LDLR is apolipoprotein E (apoE), a 299-amino acid residue, two-domain protein [11] consisting of a large globular part, which contains the LDLR recognition site in the sequence 136–150, and a lipid-binding region for anchorage within the lipoprotein. Lipoprotein-like particles prepared by complexing apoE with liposomes are successfully used for tumor-specific drug application [12–15]. Drugs that have been efficiently transported across the BBB using apoE-coated nanoparticles include the analgetic hexapeptide dalargin and the tumor therapeutic doxorubicin [16,17].

Although the entire apoprotein can be applied for carrier modification, truncated sequences containing only the residues required for receptor binding might be used advantageously. Thus, synthetic peptides such as the tandem dimer (141–150)₂ were found to compete with LDL for receptor binding [18] and to induce endocytosis in cultivated cortical neurons [19]. However, when the peptide is covalently bound to the polar surface of polyethyleneglycol-coated liposomes, uptake of the complex into cells is determined by an LDLR-independent mode [20]. Most likely, the peptide located in the rather polar environment is not able to assume the helical structure that has been suggested to be a prerequisite for receptor recognition [18]. In contrast, peptides encompassing the whole or larger parts of the receptor-binding region of apoE (136–150) and modified with one or two fatty acid chains [21] as well as an apoE peptide linked to a class-A amphipathic peptide [22,23] associate with LDL and likely involve the LDL receptor in the cellular uptake process.

Thus, in addition to the development of the target recognition moiety, the optimization of strategies for its coupling to the carrier is another important element in the development of drug delivery systems. One approach to coat liposomes with apo E-derived peptides and to induce the LDLR-competent structure relies on adsorptive binding to the liposomal surface. We prepared two-domain peptides by modifying the tandem dimer (141–150)₂ with C-terminally coupled amphipathic or highly hydrophobic helices known to assume an in-plane orientation at the lipid bilayer [24] or acting as transmembrane building blocks of many membrane proteins [25], respectively. Furthermore, one or two acyl chains, which serve to promote membrane anchorage and function of several proteins [26,27], were coupled to the N-terminus of the vector sequence. In this study, we investigated how the different lipid-associating domains affect lipid binding, structure, stability of anchorage, bilayer-disturbing activity and toxicity of the apoE peptide. The main aim was to determine the peptide derivative which is anchored at the surface of the liposome in a receptor-accessible way without deterioration of the vesicle structure on a physiologically relevant time scale. A combined approach of applying different physical methods such

as fluorescence spectroscopy, circular dichroism (CD) spectroscopy, isothermal titration calorimetry (ITC) and a toxicity assay indicates that complexes of the dipalmitoylated apoE derivative with liposomes seem to be the most promising delivery system combining the purposes of a stable drug container and of targeting the blood–brain barrier. Confocal laser scanning microscopic studies revealed the efficient internalization of the peptide–liposome complexes into brain capillary endothelial cells.

2. Materials and methods

2.1. Materials

Protected amino acids were purchased from Novabiochem (Bad Soden, Germany). Palmitic acid, myristic acid and other chemicals and solvents used for peptide synthesis were from Fluka (Buchs, Switzerland). The lipids 1-palmitoyl-2-oleoyl-*sn*-glycero-3-phosphocholine (POPC), 1,2-dipalmitoyl-*sn*-glycero-3-phosphoethanolamine-*N*-[lissamine rhodamine B sulfonyl] (Rh-DPPE), 1-palmitoyl-2-stearoyl-(5-DOXYL)-*sn*-glycero-3-phosphocholine (5-DOX), 1,2-dioleoyl-*sn*-glycero-3-phospho(TEMPO)choline (TEMPO), and 1-palmitoyl-2-stearoyl-(6-7)dibromo-*sn*-glycero-3-phosphocholine (DiBr-PSPC) were purchased from Avanti Polar Lipids (Alabaster, USA). Calcein was obtained from Fluka (Neu-Ulm, Germany) Tris(hydroxymethyl)aminomethane (Tris), trifluoroethanol (TFE), and other chemicals used for biophysical experiments were from Merck (Darmstadt, Germany). The tissue culture media Alpha-medium/Ham's F-10 (1/1 v/v), Earle's minimal essential medium, fetal bovine serum, penicillin/streptomycin, and L-glutamine were from Biochrom (Berlin, Germany), and fibroblast growth factor and rat tail collagen were from Roche Diagnostics (Mannheim, Germany). (3-(4,5-dimethylthiazol-2-yl)-2,5-diphenyl)tetrazolium bromide (MTT) was obtained from Sigma (Deisenhofen, Germany).

2.2. Peptide synthesis and characterization

The peptides were synthesized on solid phase (TentaGel-S-RAM; Rapp Polymere, Tübingen, Germany) using an ABI 433A automatic peptide synthesizer (Applied Biosystems, Foster City, USA) following the standard Fmoc (9-fluorenylmethoxycarbonyl) chemistry protocol [28]. The peptides were C-terminally amidated. N-terminal acylation was performed either with acetic acid or, in the case of P2A2, PA2 and MA2, with palmitic and myristic acid, respectively. Acylation was performed with diisopropylcarbodiimide and *N*-hydroxybenzotriazole overnight. The dipalmitoylated peptide P2A2 was synthesized using a Dde-protected Fmoc-lysine derivative (N^ε-(9-fluorenylmethoxycarbonyl)-N^ε-1-(4,4-dimethyl-2,6-dioxocyclohex-1-ylidene)ethyl-L-lysine). After coupling of the final tryptophan, the Dde and the N-terminal Fmoc groups were cleaved off with 2% hydrazine in dimethyl formamide for 10 min. The two amino groups of the resin-bound peptide (~50 μmol) were acylated overnight with a 10-fold excess of palmitic acid activated with diisopropylcarbodiimide/*N*-hydroxybenzotriazole. Cleavage from the resin with 10% phenol in trifluoroacetic acid (TFA) for 3 h gave the C-terminally amidated peptides. The crude peptide products were precipitated in diethyl ether and lyophilized from 10% acetic acid. Purification was carried out by preparative high-performance liquid chromatography (HPLC) using an LC-10AD system (Shimadzu, Kyoto, Japan) operating at 220 nm, yielding a purity better than 95% as determined by analytical reversed-phase HPLC on an LC-10AD instrument (Jasco, Germany) using an A300 Polycap column (250 × 20 mm; Bischoff Analysentechnik und -geräte, Leonberg, Germany) and a flow gradient of 10 mL/min with 40–95% B (80% acetonitrile, 20% H₂O, 0.1% TFA) in A (0.1% TFA in H₂O for 70 min). The compounds were further characterized by matrix-assisted laser desorption/ionization time-of-flight mass spectrometry (MALDI-TOF) on a Voyager-DE STR (Applied Biosystems, Foster City, USA).

2.3. Liposome preparation

Small and large unilamellar vesicles (SUVs and LUVs, respectively) were prepared as described elsewhere [29]. The dry lipid films were suspended by

vortexing in 10 mM Tris buffer (pH 7.4) containing 0.1 mM EDTA and 154 mM NaF or NaCl for spectroscopic or other experiments, respectively. SUVs were made by sonification of the liposome suspension with a Labsonic L instrument (B. Braun, Melsungen, Germany). LUVs were prepared by 35 extrusion steps through two stacked polycarbonate filters with 100-nm pores using a MiniExtruder (Avestin, Ontario, Canada). The vesicle size checked on a Coulter N4 Plus particle sizer (BeckmanCoulter, Fullerton, USA) was found to be narrowly centered around 35 nm for SUVs and 100 nm for LUVs, respectively. The lipid concentration was determined by phosphorous analysis [30]. Peptide–liposome complexes were prepared by mixing both components at appropriate concentrations.

2.4. Circular dichroism spectroscopy

Circular dichroism (CD) measurements of peptides dissolved at 20 μ M in buffer (10 mM Tris, 154 mM NaF, 0.1 mM EDTA, pH 7.4), in buffer/TFE (1/1 v/v) and in 1 mM POPC SUV suspensions were carried out on a J 720 spectrometer (Jasco, Tokyo, Japan). CD and differential scattering of the SUVs were eliminated by subtracting the spectra of the corresponding peptide-free lipid suspensions. The presented spectra give the mean residual ellipticity, $[\Theta]$, of one out of three independent experiments. The peptide helicity, α , was calculated from the mean residual ellipticity at 222 nm, Θ_{222} , according to the equation α (%) = $-(\Theta_{222} + 2340)/30300 \times 100\%$ [31]. The standard error in helicity was $\leq 5\%$.

2.5. Fluorescence and quenching studies

Fluorescence measurements were made on an LS 50B spectrofluorimeter (Perkin Elmer, Rodgau-Jügesheim, Germany). Stock peptide solutions were prepared in buffer (10 mM Tris, 154 mM NaCl, 0.1 mM EDTA, pH 7.4). POPC-SUVs containing different amounts of the fluorescence-quenching lipid DiBr-PSPC (0–60 mol%) were prepared as described above. Aliquots of the peptide solutions were mixed in a 1-cm² fluorescence cell (Hellma, Müllheim, Germany) with either buffer or liposome suspensions to give the final peptide concentration of 2 μ M and a total lipid concentration of 2 mM with an increasing content of the quencher-bearing lipid. Solutions for baseline samples lacked peptide. Peptide–vesicle interactions were recorded by measuring the tryptophan fluorescence excited at 285 nm (slit width = 5 nm) between 300 nm and 480 nm (slit width = 5 nm).

The kinetic stability of peptide–liposome complexes was determined in redistribution experiments. Aliquots of the peptide stock solutions and POPC SUV suspensions containing 40 mol% DiBr-PSPC were mixed in a cuvette to give a peptide and lipid concentration of 2 μ M and 2 mM, respectively, at 2500 μ L sample volume. After 30 min of incubation the fluorescence intensities of the lipid-bound peptides were determined at the wavelength of the emission maximum. After addition of 100 μ L quencher-free 40 mM SUV suspension, the final lipid concentration was 3.8 mM. The fluorescence was registered at time intervals over a period of another 30 min and corrected for dilution and background signals of peptide-free suspensions. Redistribution of peptides to quencher-free vesicles was monitored as an increase in the fluorescence intensity, whereas no intensity change was observed with kinetically stably anchored peptides.

To determine the depth of insertion of the apoE peptides into the lipid bilayer, fluorescence quenching experiments using nitroxide-labeled PC (TEMPO, 5-DOX) were carried out as described elsewhere [32]. The peptides were dissolved in ethanol. 20 μ L of the 200 μ M solution was given into the lipid-containing tube to dissolve the lipid film followed by vortex mixing with 1980 μ L buffer (10 mM Tris, 154 mM NaCl, 0.1 mM EDTA, pH 7.4). The final concentrations were 200 μ M lipid and 2 μ M peptide, and the content of TEMPO or 5-DOX ranged from 0 to 40 mol%. The tryptophan fluorescence excited at 285 nm was measured at 344 nm. Parallax analysis was performed as described elsewhere [33,34]. The distance of the tryptophan chromophore from the bilayer center, z_{cf} , was calculated using the equation $z_{\text{cf}} = L_{\text{c1}} + [-\ln(F_1/F_2)/\text{PIC} - L_{21}]/2 L_{21}$, with L_{c1} being the distance of the shallow quencher from the bilayer center, F_1 and F_2 the fluorescence intensities in the presence of the shallow or deeper quencher, respectively, and L_{21} the difference in depth between the shallow and the deeper quencher. C is the mole fraction of quencher divided by the cross-sectional area of a lipid, which is 70 Å². The distances of the quenching groups from the bilayer center have been reported to be 19.5 Å for TEMPO [33] and 12.2 Å for 5-DOX [34].

2.6. Isothermal titration calorimetry

Isothermal titration calorimetry (ITC) was performed on a VP instrument (MicroCal, Northampton, USA). Experiments were made with SUVs at 25 °C. 10 μ L aliquots of the suspension (lipid concentration $c_l = 40$ mM) were injected to the peptide solution (concentration $c_p = 20$ μ M) in the calorimeter cell ($V = 1.3998$ mL). From the sum of the heat of injections, the reaction enthalpy, ΔH , was calculated. The heat of reaction as a function of the molar amount of injected lipid was used to calculate binding isotherms. The evaluation of such data sets has been explained elsewhere [35]. Binding of the cationic peptides to SUVs can be described by a surface partition equilibrium with the condition that the extent of peptide adsorption is linearly related to the peptide concentration at the vesicle surface, c_b : $R_b = K \times c_b$. R_b is the molar amount of peptide bound per mole of lipid, and K is the intrinsic binding constant. c_b depends on the free peptide concentration in the bulk solution, on the peptide charge, and on the membrane surface potential, which can be calculated with the aid of the Gouy–Chapman theory [36]. After derivation of K from the experimental data, the standard Gibbs free energy change, ΔG° , and the change in standard entropy, ΔS° , were available via the relations $\Delta G^\circ = -RT \ln(K \times 55.5 \text{ M})$ and $\Delta G^\circ = \Delta H^\circ - T\Delta S^\circ$, respectively. R stands for the universal gas constant and T for the absolute temperature. The molar concentration of water (55.5 M) corrects for the fact that the bound peptide is given as molar ratio, whereas the aqueous peptide concentration is given as molarity.

2.7. Dye release from liposomes

Peptide-induced bilayer permeabilization was monitored fluorimetrically by measuring the decrease in self-quenching of vesicle-entrapped calcein as described previously [29]. LUVs were prepared in buffered dye solution (70 mM calcein, 10 mM Tris, 0.1 mM EDTA, pH 7.4). Calcein fluorescence excited at 490 nm was registered at 520 nm as a function of time using an LS 50B spectrofluorimeter (Perkin Elmer, Rodgau-Jügesheim, Germany). The peptide concentration ranged from 1 to 100 μ M, the lipid concentration was 25 μ M. The fluorescence intensity corresponding to 100% dequenching was determined by addition of Triton X-100 (10% v/v in water). EC_{50} is the peptide concentration inducing half-maximal dye release 5 min after peptide addition to the liposome suspension.

2.8. Cell viability

Peptide toxicity was monitored by the MTT method as described before [20]. Rat brain capillary endothelial cells, RBE4 [37] were cultured in Alpha-medium/Ham's F-10 (1/1 v/v) containing 10% (v/v) fetal bovine serum, 1% (v/v) penicillin/ streptomycin (10 000 μ g/mL), 2 mM L-glutamine and 1 ng/mL fibroblast growth factor. 25 000 cells per well were seeded 48 h prior to the experiment in a rat tail collagen-coated 96-well plate. After the medium was removed, the cells were exposed to 200 μ L increasing concentrations of apoE peptides in growth medium for 30 min at 37 °C. After washing, addition of 180 μ L fresh medium and 20 μ L MTT solution in 5 mg/mL phosphate-buffered saline (PBS) per well, and incubation the cells for 4 h at 37 °C, the medium was replaced with 100 μ L DMSO/well. Cell viability was quantified by measuring the optical density at 550 nm and 650 nm as reference using a microplate reader (Tecan Safire, Männedorf, Switzerland). Absorption determined with untreated cells was taken as 100% cell viability.

2.9. Cellular uptake

POPC LUVs for cellular uptake studies were prepared with Dulbecco's phosphate-buffered saline (PBS) containing Ca^{2+} , Mg^{2+} , and 1 mg/mL D-glucose. Aliquots of the vesicle suspension were mixed with the P2A2 solution to give a final lipid concentration of 1 mM and peptide concentration of 1 μ M. The complexes contained 0.1 mol% LissamineTM rhodamine B 1,2-dipalmitoyl-sn-glycero-3-phosphoethanolamine (Rh-DPPE) in the lipid bilayer or 400 μ M fluorescein isothiocyanate-dextran WT 4000 (FITC-dextran) inside the vesicles. Immortalized b.End3 mouse brain capillary endothelial cells [38] were cultured in a humidified atmosphere (37 °C, 5% CO_2) with Earle's minimal essential medium supplemented with 10% fetal bovine serum, 2 mM N-acetyl-L-alanyl-L-

Table 1
Sequences of apoE peptides

Abbreviation	Sequence
A2	Ac-(LRKLRKRLLR) ₂ -NH ₂
A2Q	Ac-(LRKLRKRLLR) ₂ PLVEDMQRQWAGLV-NH ₂
A2T	Ac-(LRKLRKRLLR) ₂ AWLALALALALKALALALALKK-NH ₂
MA2	myristoyl-WAG(LRKLRKRLLR) ₂ -NH ₂
PA2	palmitoyl-WAG(LRKLRKRLLR) ₂ -NH ₂
P2A2	palmitoyl-WK(palmitoyl)G(LRKLRKRLLR) ₂ -NH ₂

glutamine, 100 units/mL penicillin, and 100 µg/mL streptomycin. For microscopic studies, cells were plated on poly-L-lysine-coated glass coverslips and maintained under the same conditions. After 3 days, the cells were washed with PBS and exposed to the vesicle suspension for 30 min at 37 °C followed by three washing steps with ice-cold PBS. Fluorescence images were taken using an LSM 510 META inverted confocal laser scanning microscope equipped with a Plan Neofluar 100x/1.3 Oil objective a helium/neon laser with a dichroitic HTF mirror, and an argon laser with a DPS1 mirror (Carl Zeiss, Jena, Germany). Upon excitation at 543 nm with the He/Ne laser, rhodamine emission was registered using an LP 560 cutoff filter in front of the detector. FITC was excited at 488 nm with the argon laser, and CLSM images were taken with a BP 505–530 bandpass filter. After each experiment, membrane integrity and cell viability were ensured by trypan blue staining.

3. Results

3.1. Peptide design and synthesis

Based on the two-domain structure of apolipoprotein E, two-domain apoE peptides were synthesized (Table 1). The peptides consist of the tandem dimer of residues 141–150 of apoE (A2) shown to compete with LDL for binding to LDLr [18,20]. A2 is characterized by a low hydrophobicity of $H = -0.73$, and its ideal helix has a high hydrophobic moment of $\langle \mu \rangle = 0.4$ as calculated using the Eisenberg consensus scale for hydrophobicity [39]. The amphipathic helix, Q, corresponds to the sequence 267–280 of the lipid-associating region of apoE [40]. The hydrophobic sequence, T, is analogous to helical peptides adopting a transmembrane orientation in lipid bilayers [41–43]. M and P represent myristoyl and palmitoyl chains, respectively, the most common forms of protein acylation [26] and frequently used to promote peptide association with lipid bilayers [44]. The expected localizations of A2Q, A2T, and the dipalmitoylated P2A2 in lipid vesicles are schemed out in Fig. 1. All peptides contain

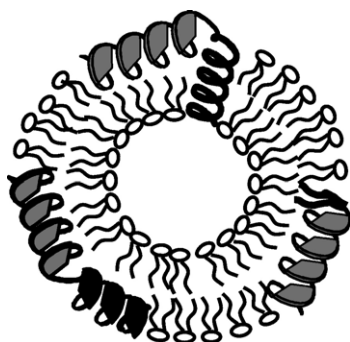


Fig. 1. Different noncovalent ways of anchoring two-domain apoE peptides in lipid bilayers.

one tryptophan residue, the fluorescence of which is highly sensitive to the environment and used to monitor peptide–lipid interactions [45].

3.2. Circular dichroism spectroscopy

As helix formation seems to be a prerequisite for the recognition of the LDL receptor by apoE peptides [46] peptide conformation was examined using circular dichroism spectroscopy. The CD spectra of A2, A2Q (Fig. 2A), MA2 and PA2 dissolved in buffer characterize highly flexible chains. The helical content was less than 10% (Fig. 2B). A slightly enhanced helicity of P2A2 pointed to the formation of micelles as confirmed by light scattering and ultracentrifugation experiments [47]. The high helix content of A2T at 20 µM concentration probably was due to peptide association mediated by the hydrophobic transmembrane sequence [42]. CD spectra characterized by minima at 207 and 222 nm (Fig. 2A) and helicities greater than 75% (Fig. 2B) in structure-inducing TFE/buffer mixtures pointed to the pronounced ability of all peptides to adopt an α -helical structure. In the presence of POPC vesicles, A2 showed only minor structural changes, indicative of weak interactions with the lipid bilayer.

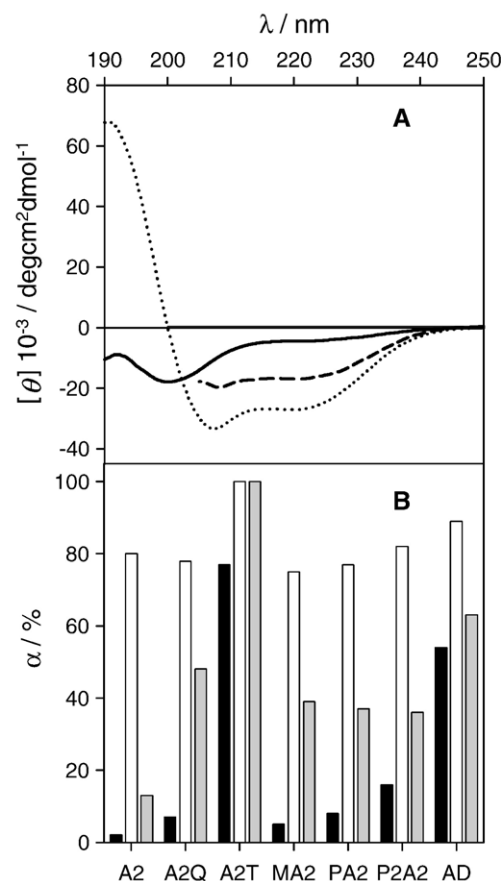


Fig. 2. CD characteristics and helicities of apoE peptides. (A) CD spectra of 20 µM A2Q in buffer (solid line), in buffer/TFE (1/1 v/v) (dotted line), and in the presence of 1 mM POPC SUVs (dashed line). $[\Theta]$ is the mean residual ellipticity. (B) Helicity, α , of apoE peptides in buffer (black), in buffer/TFE (1/1 v/v) (white), and in the presence of 1 mM POPC SUVs (grey). The peptide concentration was 20 µM.

Table 2
Physicochemical properties of apoE peptides

Peptide	λ_{\max} (nm)	F_{\max} (au)	λ_{\max} (nm)	F_{\max} (au)	K (mM ⁻¹)	EC ₅₀ (μ M)	c_l/c_p
	Buffer		POPC				
A2	n.a.	n.a.	n.a.	n.a.	n.a.	0.03	833
A2Q	354	64	335	62	17	0.02	1250
A2T	333	110	332	127	n.d.	0.04	625
MA2	352	58	342	102	30	0.02	1250
PA2	350	61	342	110	30	0.01	2500
P2A2	344	39	342	86	>>1000	0.06	417

The fluorescence properties of 2 μ M W-containing peptides were determined in Tris buffer and in the presence of POPC-SUVs (lipid concentration $c_l=2$ mM). Fluorescence was excited at 280 nm (λ_{\max} , wavelength of the emission maximum; F_{\max} , fluorescence intensity at λ_{\max}). The partition coefficient, K , was derived from ITC measurements. POPC-SUVs ($c_l=30$ mM) were titrated into 20 μ M peptide solutions in Tris buffer (n.d., not determined; n.a., not applicable). EC₅₀ is the half-maximal peptide concentration needed to induce dequenching of the fluorescence of calcein entrapped in POPC-LUVs ($c_l=25$ μ M) taken 5 min after the addition of peptide, and c_l/c_p gives the corresponding lipid-to-peptide ratio.

Sequence modification with lipid-associating domains led to liposome binding and distinctly increased helicity (Fig. 2A, B). As shown for MA2, PA2, and P2A2, the tandem dimer A2 assumed about 40% helicity in the vesicle-bound state. Higher helicities of A2Q and A2T might be associated with the elongation of the peptide helix caused by the extension of the nonpolar face of A2 with the lipid-associating sequences [22].

3.3. Fluorescence spectroscopy

Tryptophan residues fully exposed to an aqueous environment have maxima above 350 nm, whereas those that are partially or completely shielded have maxima below 345 nm and at 332 nm, respectively [45]. The fluorescence maxima of A2Q, the monoacylated MA2 and PA2 dissolved in buffer above 350 nm are indicative of an aqueous environment of their tryptophan residues (Table 2). The shifts in the maxima to shorter wavelengths and the intensity increases in the presence of POPC vesicles suggested that the aromatic residues became buried in the hydrophobic region of the lipid bilayer. Maxima at 343 and 333 nm of buffer-dissolved P2A2 and A2T, respectively pointed to pronounced shielding of the chromophor from the polar environment as result of association (Table 2). Detection of their interaction with liposomes on the basis of environment-dependent spectroscopic changes was not possible. Therefore, the fluorescence was measured in the presence of quencher-bearing lipid vesicles. As shown in Fig. 3, all peptides showed a comparable reduction in the emission intensity with increasing amounts of DiBr-PSPC, indicating that also A2T and P2A2 were bound to the lipid membrane.

To determine the kinetic stability of peptide anchoring within the lipid bilayer, fluorescence dequenching caused by desorption from quencher-bearing liposomes was monitored. Addition of quencher-free POPC SUVs to a A2Q-liposome suspension containing 40 mol% DiBr-PSPC led to an immediate intensity increase as the peptide was rapidly redistributed (Fig. 4). Over a period of 30 min no further change was monitored. The same

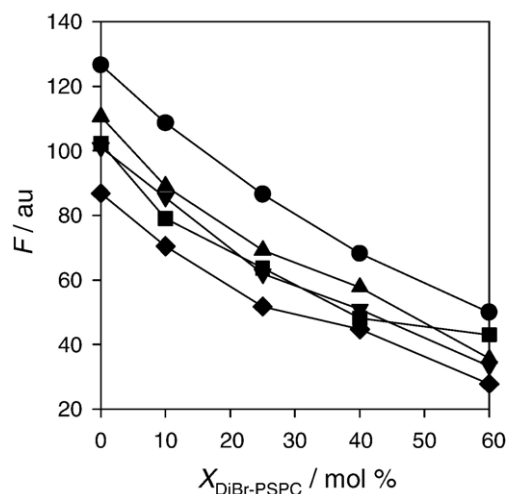


Fig. 3. Fluorescence intensities, F , of A2Q (squares), A2T (circles), MA2 (down triangles), PA2 (up triangles), and P2A2 (diamonds) bound to POPC vesicles in dependence of the mole fraction, X , of the quencher-labeled lipid DiBr-PSPC. The peptide concentration was 2 μ M, the lipid concentration 2 mM. The intensities were registered at the wavelength of the emission maximum, λ_{\max} (Table 2).

transferability was observed for magainin 2 amide (data not shown), an amphipathic helical peptide with low affinity to neutral POPC bilayers [48]. Whereas PA2 and even A2T slowly redistributed over a period of 30 min as shown by the slight time-dependent increase in fluorescence intensity after SUV addition, almost no change was observed for P2A2, suggesting that the dipalmitoylated peptide was kinetically stably anchored within the vesicle bilayer. The observation is in accordance with the suggestion that a second palmitoyl anchor is needed for stable membrane attachment of proteins [26].

To determine the position of the two peptides A2T and P2A2 in the lipid bilayer, fluorescence quenching experiments using

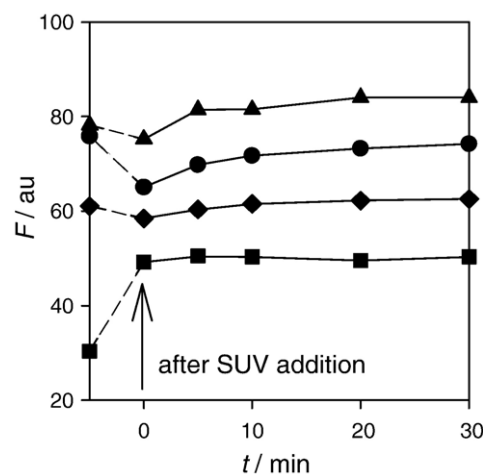


Fig. 4. Fluorescence intensities, F , of A2Q (squares), A2T (circles), PA2 (up triangles), and P2A2 (diamonds) bound to POPC/DiBr-PSPC (60/40 mol/mol; lipid concentration 2 mM) measured at the wavelength of the emission maximum, λ_{\max} , and in dependence of time after addition of POPC SUVs (arrow). The final lipid concentration was 3.8 mM, and the peptide concentration was 2 μ M.

Table 3
Quenching of the tryptophan fluorescence by nitroxide-labeled lipids and distance of W from the POPC bilayer center

Peptide	S		z_{cf} (Å)
	TEMPO	5-DOX	
A2T	−2.89	−3.92	14.3
P2A2	−3.31	−4.24	14.4

S is the slope of the plot of $\ln(F/F_0)$ versus the mole fraction of lipids carrying the nitroxide label at 19.5 Å (TEMPO) or 12.2 Å (5-DOX) from the bilayer center. F/F_0 is the ratio of the fluorescence intensity in the presence of POPC vesicles containing the quencher to that of vesicles without the quencher. The mole fraction of labeled lipid ranged from 0 to 0.4. The peptide concentration was 2 μM , the lipid concentration was 400 μM . The distance of the tryptophan residue from the bilayer center, z_{cf} , was calculated by applying the parallax equation [33,34].

nitroxide-labeled lipids were carried out. Quenching is most efficient and the parallax analysis is most accurate when the chromophore is close to the quencher [49]. The S -values summarized in Table 3 give the slopes of the plots of $\ln(F/F_0)$

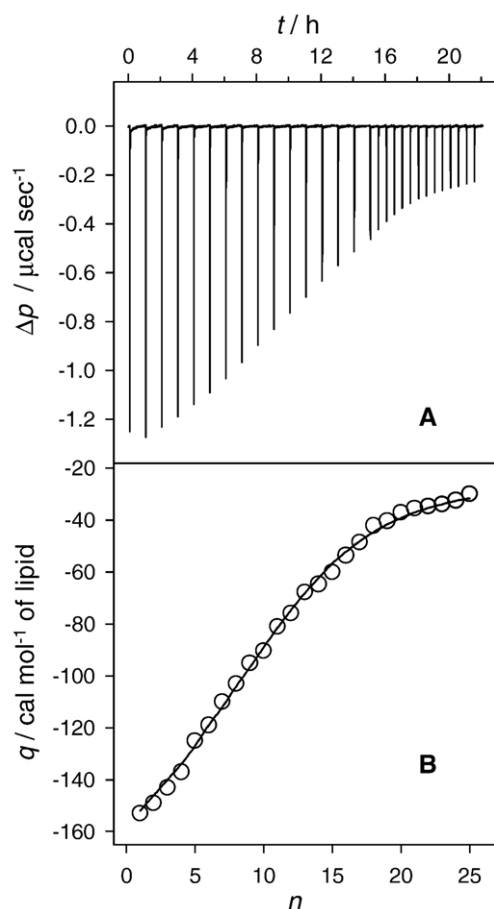


Fig. 5. Titration calorimetry of 20 μM A2Q solutions with a POPC SUV suspension (lipid concentration 40 mM; volume of injection 10 μL) at 25 $^{\circ}\text{C}$. (A) The calorimetric trace gives the heat flow, Δp , versus time, t . (B) The heat of reaction per mole of injected lipid, q , as a function of the injection number, n , was obtained by integration of the peaks in (A). The fitted curve was calculated by combining a surface partition equilibrium with the Gouy–Chapman theory and corresponds to a binding constant of $K=17 \text{ mM}^{-1}$ (Table 2).

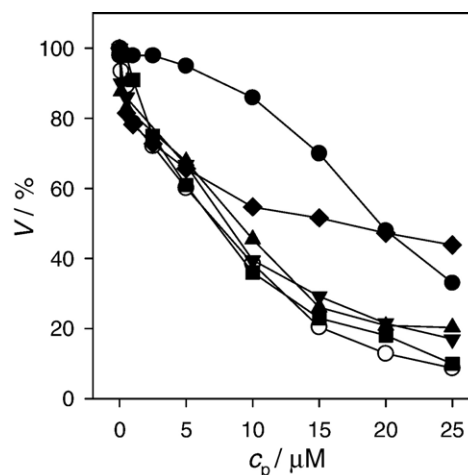


Fig. 6. Viability, V , of rat capillary endothelial cells (RBE4) in dependence of the concentration of A2 (open circles), A2Q (squares), A2T (circles), MA2 (down triangles), PA2 (up triangles), and P2A2 (diamonds).

versus the mole fraction of labelled lipid and are a measure of the quenching efficiencies of TEMPO- and 5-DOX-labeled lipids on POPC-bound peptides. The calculated distance from the bilayer centre, z_{cf} , was 14.4 Å for tryptophan located at the acylated N-terminus of P2A2 and 14.3 Å for the chromophore positioned between the A2 sequence and the transmembrane helix in A2T. Thus, both chromophores are located next to the head group-acyl chain interface and the adjacent A2 domains are likely exposed to the surface.

3.4. Isothermal titration calorimetry

Peptide binding was quantified by isothermal titration calorimetric studies. Results from a typical experiment are shown in Fig. 5. The exothermic heats of reaction decreased with consecutive POPC SUV injections into the A2Q solution because less and less peptide was available for binding (Fig. 5A). Towards the end of the experiment, the heats of reaction given in Fig. 5B approached the constant heat of dilution, indicating that almost all peptide was bound to the vesicles. For A2Q, the molar transfer enthalpy from the aqueous solution into the lipid bilayer was determined to be $\Delta H = -21.4 \text{ kcal mol}^{-1}$, and the hydrophobic partition coefficient was $K = 17 \text{ mM}^{-1}$. The standard Gibbs free energy change upon partitioning was calculated as $\Delta G^{\circ} = -8.2 \text{ kcal mol}^{-1}$, and the standard entropy change was $\Delta S^{\circ} = -44.5 \text{ cal mol}^{-1} \text{ K}^{-1}$. Thus, binding of the amphipathic peptide to POPC vesicles is an enthalpy-driven reaction opposed by entropy. Hydrophobic binding constants derived for the investigated two-domain peptides are summarized in Table 2. The lipid affinity of the highly positively charged unmodified A2 could not be determined as the ITC signals did not exceed typical heats of dilution. The partitioning of P2A2 between the aqueous and the bilayer phase could not be quantified because of the low monomeric solubility, but other titration calorimetric studies imply that the partition constant is much higher than 10^6 M^{-1} [47].

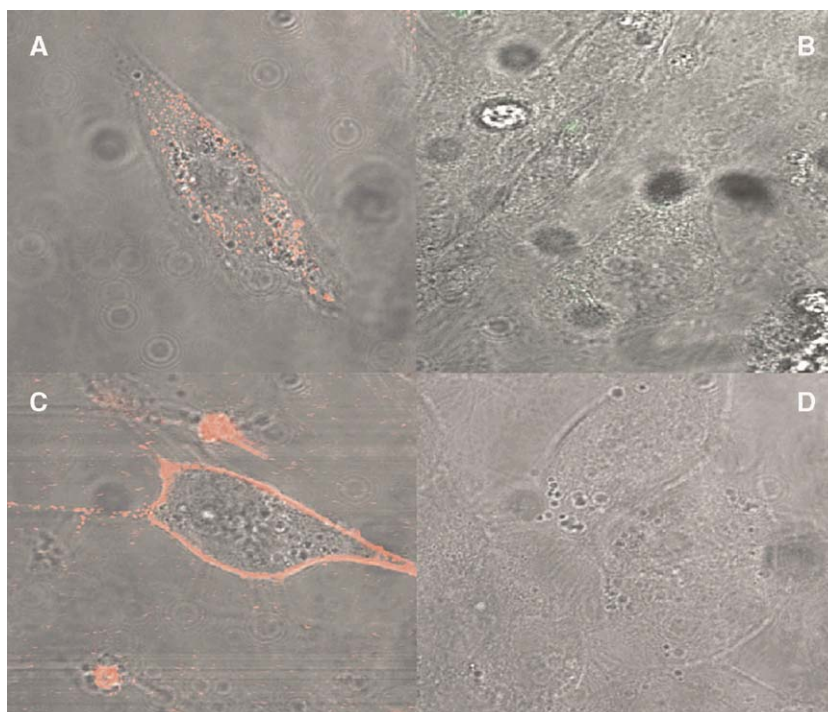


Fig. 7. CLSM pictures of mouse brain capillary endothelial cells (b.End3) incubated with Rh-DPPE-doted P2A2-liposomes (A), FITC-dextran-containing P2A2-vesicles (B) and blank liposomes (D) for 30 min at 37 °C and exposure to Rh-DPPE-doted P2A2-liposomes for 30 min at 4 °C (C). The lipid concentration was 1 mM, the molar peptide-to-lipid ratio was 1000 and the FITC-dextran concentration was 400 μ M. Punctuated intracellular fluorescence (A, B) at 37 °C and membrane accumulation (C) at 4 °C point to a predominant endocytotic mode of uptake of the intact liposomes. Membrane integrity and cell viability were confirmed by trypan blue exclusion (not shown).

3.5. Vesicle permeabilization

Surface-active amphipathic peptides are able to perturb lipid bilayers at sufficiently high concentrations rendering the liposomal carrier leaky. With an EC_{50} value of 0.03 μ M, the bilayer-permeabilizing activity of A2 is rather high. Coupling of lipid-associating domains had only a minor influence on the activity, except for the P2 modification, which tended to reduce the bilayer-disturbing effect (Table 2). Half maximal dye release was observed at a lipid-to-P2A2 ratio of about 400. The results suggest that permeabilization is dominated by the highly cationic A2 helix and that the lipid-binding domains do not provide an additional membrane-destabilizing contribution.

3.6. Cytotoxicity

The toxicity of cationic peptides is dose limiting in biological applications. We investigated the effect of the peptides and P2A2–liposome complexes on cells in a toxicity assay detecting the dehydration of the MTT reagent by mitochondrial dehydrogenase after destruction of the cell envelope. The peptides caused toxicity of rat brain capillary endothelial cells at micromolar peptide concentrations (Fig. 6). Cell survival was reduced to 80% at 2 μ M A2, A2Q, MA2, PA2, and P2A2. Less toxic than the other sequences were A2T and P2A2 at higher peptide concentrations. This decrease in cytotoxicity correlated well with the slightly reduced bilayer permeabilization caused by these two peptides (Table 2).

3.7. Cellular uptake

Limited by the bilayer-permeabilizing and toxic activities, the lipid-to-apoE peptide ratio of complexes used in cell biological studies must not fall below about 400. As shown in Fig. 7, P2A2-modified liposomes (diameter \sim 100 nm) prepared at a molar lipid-to-peptide ratio of 1000 and thus containing about 180 peptide molecules on the surface were efficiently internalized into mouse brain capillary endothelial cells when incubated at 37 °C. Both peptide-doted vesicles labeled with Rh-DPPE within the lipid bilayer (Fig. 7A) or FITC-dextran dissolved in the aqueous lumen (Fig. 7B) accumulated in distinct intracellular compartments, suggesting that the intact particles are taken up by an endocytotic process. Abolished uptake and cell surface accumulation at 4 °C (Fig. 7C) supported the suggestion. Cells treated with liposomes without P2A2 modification showed neither intracellular nor membrane-associated fluorescence (Fig. 7D).

4. Discussion

A fundamental understanding of the interplay between the lipid bilayer of liposomes and vector peptides is crucial for the use of the complexes as potential carriers in drug targeting. To investigate the most efficient way of coating liposomes by adsorptive coupling of an apoE-derived LDL-receptor recognition peptide, we compared peptides modified with an amphipathic and transmembrane helix, a single fatty acid chain, or a dipalmitoyl modification as vesicle anchors. The following order in the

properties of the peptide considered relevant to the vector liposome complexes as pharmaceutical formulations emerged:

Binding to liposomes :

$$A2 \ll A2Q < MA2 = PA2 \ll P2A2$$

Stability of anchorage :

$$A2Q \ll PA2 < A2T < P2A2$$

Helicity :

$$A2 < MA2 = PA2 = P2A2 < A2Q < A2T$$

Permeabilizing activity :

$$A2Q = A2M = A2P \geq A2 \geq A2T > P2A2$$

Toxicity :

$$A2 = A2Q \geq MA2 = PA2 > P2A2 \geq A2T$$

The results suggest that the dipalmitoylated peptide, P2A2, is most promising to prepare complexes with liposomes that are stable on time scales relevant for biological application and to mediate an efficient uptake into brain capillary endothelial cells.

Binding and CD spectroscopic studies demonstrating a low affinity to neutral lipid surfaces and a high conformational flexibility of A2 in aqueous solution are in agreement with previous investigations of the sequence (129–169) [21] and (141–150) [22]. Modifications of A2 by covalent attachment of lipid-associating moieties served two purposes. First, they increased the affinity of the peptides to the liposomal surface, and second, the bound peptides folded into a helix.

As reported for many amphipathic helices of different primary structure [48], A2Q undergoes a disordered-helix transition while binding to the lipid bilayer. However, the low binding constant and the immediate intervesicle transfer of the peptide upon addition of liposomes to a suspension of peptide liposome complexes suggest that the amphipathic sequence 267–280 of the lipid-associating region of apoE [40] is not sufficient to fully anchor the receptor binding sequence within the liposome. Thus, despite pronounced helicity and unmodified lytic and toxic activity, A2Q is not suitable to generate liposomal delivery systems.

Myristoyl and palmitoyl chains distinctly enhanced the lipid affinity of A2. Unlike less cationic monoacylated peptides such as magainin analogs [50] or proteins modified with myristoyl or palmitoyl groups [51], which tend to form micelles in aqueous solution in dependence of concentration, no self-association of the two peptides was observed at 2 μ M, the upper concentration for cell experiments imposed by cytotoxicity. Systematic studies of the effect of the acyl chain length on peptide affinity to lipid membranes have shown that the Gibbs free energy of binding of -8 kcal/mol provided by myristoyl [52] is insufficient to fully anchor a peptide in the lipid bilayer. Even prolongation of the acyl chain by two methylene units, decreasing the free energy of binding by about -0.7 kcal/mol [53], is insufficient for kinetically stable anchorage of the cationic A2 sequence in the surface of liposomes composed of zwitterionic lipids.

For basic amino acid domains of proteins, electrostatic interactions with anionic lipids in the membrane or a second palmitoyl anchor have been proposed for stable membrane attachment [26].

Indeed, dipalmitoyl modification of A2 pronouncedly increases binding to lipid membranes. A thermodynamic description of the interactions with liposomes shows that the peptide remains anchored in the lipid bilayer above a molar lipid-to-peptide ratio of about 80, and at lower ratios the kinetics of bilayer solubilization was extremely slow [47]. The derived phase diagram of P2A2–lipid interactions permitted mastery of liposomal, mixed and micellar states. As shown in this study, desorption of liposome-bound P2A2 was not detected within 30 min. This observation is in accordance with reports for other dialkylated apoE peptides [21] and sequences of lipidated protein fragments [54] and suggests that binding mediated by two N-terminally located palmitoyl chains provides complexes stable on time scales relevant for pharmacological studies. From quenching studies one can roughly estimate that the N-terminally located tryptophan of P2A2 enters the acyl region of POPC bilayers up to the third carbon. The hydrophobic gradient along the axis of an amphipathic peptide determines its inclination at the hydrophobic–hydrophilic interface and influences its mode of association with lipids [55]. Most likely, the N-terminal position of the two palmitoyl chains allows the A2 sequence to localize in the head-group acyl chain interface accessible to the cell surface located receptor.

Also, A2T forms aggregates in aqueous solution as revealed by its fluorescence and CD-spectroscopic properties. Nevertheless, the peptide shows a behavior comparable to other model transmembrane peptides [43] and partitions strongly into the lipid bilayer. The location of the sole tryptophan residue of A2T is 14.3 Å above the bilayer center. The same distance has been reported for tryptophan of the transmembrane sequence K2WL9AL9K2A [56].

Recent studies have shown that the tandem dimer of the sequence (141–155) [57] and A2 [20] recognize the LDL receptor. However, because of the lack in helicity, the affinity was much reduced compared with the natural ligand LDL. Our lipidated A2 peptides developed about 40% helicity in the lipid-bound state. As the conformation of the receptor-binding region in native apoE is helical [58], the induced helicity is expected to improve peptide interactions with the receptor.

Insertion of two-domain peptides can disturb the lipid arrangement of bilayers. Thus, bilayer permeabilization is distinctly enhanced by lipidation of the antimicrobial peptide magainin [50] and laminin-related pentapeptides [44]. At variance with such reports, the different lipid-anchoring domains discussed here have only minor influence on apoE peptide-induced bilayer permeabilization, suggesting that the high activity is determined by the A2 sequence. Comparable activities towards neutral bilayers have been reported for other cationic amphipathic model peptides [29,59] and associated with their pronounced hydrophobic moment favoring insertion into the lipid bilayer. Least active are A2T and P2A2. The disturbance of the lipid arrangement upon insertion of the A2 helix into the headgroup region may be partially compensated by the transmembrane helix or the two space-consuming acyl chains, filling the gap in the hydrophobic bilayer core. The detergent-like activity of P2A2 observed at molar lipid-to-peptide ratios lower than about 80 has been analyzed in a separate study [47].

The lipid-anchoring domains have little influence on the toxicity of the A2 peptides on capillary endothelial cells. Least toxic seem to be the A2T, P2A2 and the liposome-bound derivative, suggesting that peptide association reduces the cytotoxic effect. Comparable toxicities of A2 on capillary endothelial cells and of the tandem dimers (141–155)₂ and (141–149)₂ on T lymphocytes [60] point to a cell-type-unspecific effect. Probably, the toxic effect is mediated by strong electrostatic interactions between the highly cationic apoE sequences with negatively charged cell surface heparan sulfate proteoglycans (HSPG) as suggested for other apoE fragments [61].

The function of the P2A2 peptide as an efficient endocytosis vector was confirmed in CLSM studies with mouse brain capillary endothelial cells. The patterns of punctuated fluorescence after cell incubation with P2A2–liposome complexes were comparable to those observed for P2A2 micelles [47] as well as vesicles prepared by covalent A2 vector coupling [29]. Membrane translocation of the complex prepared by covalent A2 linkage was LDLr-independent and determined by HSPGs [29]. By contrast, Mims et al. showed that in spite of an increase of non-specific binding of LDL in the presence of the diacylated apoE peptide (129–169), a considerable greater amount of the lipoprotein was taken up in cells with upregulated LDLr than in cells with normal receptor expression [21]. Whether factors such as the size of the vesicles, the liposome composition, the surface density of the vector peptide, which all play a role in LDLr-mediated cellular responses [12,62], favor the role of HSPG as regulator of ligand–receptor encounters [63] and entail the involvement of LDLr in the cellular uptake of our P2A2 liposome complexes is presently under detailed investigation.

In summary, the dipalmitoylated apoE peptide P2A2 seems to be the most promising candidate for preparing targeting and uptake-mediating liposomal carrier systems. P2A2 is easily synthesized and characterized, and complexation with liposomes is straightforward to analyze. The hydrophobic modification fulfills the main purposes: anchorage of the peptide on the liposomal surface on an application-relevant time scale and folding into a helical receptor-binding-competent conformation without deterioration of the vesicle structure and release of content. Limited by the lytic activity, the lipid-to-apoE peptide ratio of complexes used in cell biological studies must not drop below 400, and because of cytotoxicity, the peptide concentration is limited to 2 μ M. The peptide-mediated uptake of the colloidal system emphasizes the potential of the cationic peptide as vector for improved drug delivery to the brain. The results might furthermore be used to design peptide–liposome complexes for efficient drug delivery to other targets.

Acknowledgements

We are very thankful to Dr. Michael Beyermann for helpful advises on peptide synthesis and to Heidemarie Lerch for mass spectrometric characterization of the peptides. This work was financed by the Deutsche Forschungsgemeinschaft (FG 463: grant DA 324/4-1, DA 324/4-2).

References

- [1] T.M. Allen, Liposomal drug formulations, Rationale for development and what we can expect for the future, *Drugs* 56 (1998) 747–756.
- [2] A.S. Ulrich, Biophysical aspects of using liposomes as delivery vehicles, *Biosci. Rep.* 22 (2002) 129–150.
- [3] M. Voinea, M. Simionescu, Designing of ‘intelligent’ liposomes for efficient delivery of drugs, *J. Cell. Mol. Med.* 6 (2002) 465–474.
- [4] A. Tsuji, I. Tamai, Carrier-mediated or specialized transport of drugs across the blood–brain barrier, *Adv. Drug Deliv. Rev.* 36 (1999) 277–290.
- [5] D.J. Begley, The blood–brain barrier: principles for targeting peptides and drugs to the central nervous system, *J. Pharm. Pharmacol.* 48 (1996) 136–146.
- [6] U. Bickel, T. Yoshikawa, W.M. Pardridge, Delivery of peptides and proteins through the blood–brain barrier, *Adv. Drug Deliv. Rev.* 10 (1993) 205–245.
- [7] A. Cerletti, J. Drewe, G. Fricker, A.N. Eberle, J. Huwyler, Endocytosis and transcytosis of an immunoliposome-based brain drug delivery system, *J. Drug Target.* 8 (2000) 435–446.
- [8] J. Huwyler, D. Wu, W.M. Pardridge, Brain drug delivery of small molecules using immunoliposomes, *Proc. Natl. Acad. Sci. U. S. A.* 93 (1996) 14164–14169.
- [9] B. Dehouck, M.P. Dehouck, J.C. Fruchart, R. Cecchelli, Upregulation of the low density lipoprotein receptor at the blood–brain barrier: intercommunications between brain capillary endothelial cells and astrocytes, *J. Cell Biol.* 126 (1994) 465–473.
- [10] B. Dehouck, L. Fenart, P.M. Dehouck, A. Pierce, G. Torpier, R. Cecchelli, A new function for the LDL receptor: transcytosis of LDL across the blood–brain barrier, *J. Cell Biol.* 138 (1997) 877–889.
- [11] R.W. Mahley, Apolipoprotein E: cholesterol transport protein with expanding role in cell biology, *Science* 240 (1988) 622–630.
- [12] P.C. Rensen, R.M. Schiffelers, A.J. Versluis, K.M. Bijsterbosch, M.E. Kuijk-Meuwissen, T.J. Van Berkel, Human recombinant apolipoprotein E-enriched liposomes can mimic low-density lipoproteins as carriers for the site-specific delivery of antitumor agents, *Mol. Pharmacol.* 52 (1997) 445–455.
- [13] P.C. Rensen, L.R. de Vreeh, J. Kuiper, K.M. Bijsterbosch, E.A. Biessen, T.J. Van Berkel, Recombinant lipoproteins: lipoprotein-like lipid particles for drug targeting, *Adv. Drug Deliv. Rev.* 47 (2001) 251–276.
- [14] A.J. Versluis, C.P. Rensen, E.T. Rump, T.J. Van Berkel, M.K. Bijsterbosch, Low-density lipoprotein receptor-mediated delivery of a lipophilic daunorubicin derivative to B16 tumours in mice using apolipoprotein E-enriched liposomes, *Br. J. Cancer* 78 (1998) 1607–1614.
- [15] A.J. Versluis, E.T. Rump, P.C. Rensen, T.J. Van Berkel, M.K. Bijsterbosch, Stable incorporation of a lipophilic daunorubicin prodrug into apolipoprotein E-exposing liposomes induces uptake of prodrug via low-density lipoprotein receptor in vivo, *J. Pharmacol. Exp. Ther.* 289 (1999) 1–7.
- [16] A.E. Gulyaev, S.E. Gelperina, I.N. Skidan, A.S. Antropov, G.Y. Kivman, J. Kreuter, Significant transport of doxorubicin into the brain with polysorbate 80-coated nanoparticles, *Pharm. Res.* 16 (1999) 1564–1569.
- [17] J. Kreuter, D. Shamenkov, V. Petrov, P. Ramge, K. Cychutek, C. Koch-Brandt, R. Alyautdin, Apolipoprotein-mediated transport of nanoparticle-bound drugs across the blood–brain barrier, *J. Drug Target.* 10 (2002) 317–325.
- [18] C.A. Dyer, D.P. Cistola, G.C. Parry, L.K. Curtiss, Structural features of synthetic peptides of apolipoprotein E that bind the LDL receptor, *J. Lipid Res.* 36 (1995) 80–88.
- [19] X. Wang, G. Ciraolo, G. Morris, E. Gruenstein, Identification of a neuronal endocytic pathway activated by an apolipoprotein E (apoE) receptor binding peptide, *Brain Res.* 778 (1997) 6–15.
- [20] I. Sauer, I.R. Dunay, K. Weisgraber, M. Bienert, M. Dathe, An apolipoprotein E-derived peptide mediates uptake of sterically stabilized liposomes into brain capillary endothelial cells, *Biochemistry* 44 (2005) 2021–2029.
- [21] M.P. Mims, A.T. Damule, R.W. Tovar, H.J. Pownall, D.A. Sparrow, J.T. Sparrow, D.P. Via, L.C. Smith, A nonexchangeable apolipoprotein E peptide that mediates binding to the low density lipoprotein receptor, *J. Biol. Chem.* 269 (1994) 20539–20547.

- [22] G. Datta, M. Chaddha, D.W. Garber, B.H. Chung, E.M. Tytler, N. Dashti, W.A. Bradley, S.H. Gianturco, G.M. Anantharamaiah, The receptor binding domain of apolipoprotein E, linked to a model class A amphipathic helix, enhances internalization and degradation of LDL by fibroblasts, *Biochemistry* 39 (2000) 213–220.
- [23] G. Datta, D.W. Garber, B.H. Chung, M. Chaddha, N. Dashti, W.A. Bradley, S.H. Gianturco, G.M. Anantharamaiah, Cationic domain 141–150 of apoE covalently linked to a class A amphipathic helix enhances atherogenic lipoprotein metabolism in vitro and in vivo, *J. Lipid Res.* 42 (2001) 959–966.
- [24] I. Cornut, E. Thiaudière, J. Dufourcq, The amphipathic helix in cytotoxic peptides, in: R. Epand (Ed.), *The Amphipathic Helix Concept*, CRC Press, Boca Raton, 1993, pp. 173–218.
- [25] R. von Heijne, Principles of membrane protein assembly and structure, *Prog. Biophys. Mol. Biol.* 66 (1996) 113–139.
- [26] M.D. Resh, Fatty acylation of proteins: new insights into membrane targeting of myristoylated and palmitoylated proteins, *Biochim. Biophys. Acta* 1451 (1999) 1–16.
- [27] J.R. Silvius, Lipid modifications of intracellular signal-transducing proteins, *J. Liposome Res.* 9 (1999) 1–19.
- [28] M. Beyermann, M. Bienert, Synthesis of difficult peptide sequences: a comparison of Fmoc- and Boc-technique, *Tetrahedron Lett.* 33 (1992) 3745–3748.
- [29] M. Dathe, J. Meyer, M. Beyermann, B. Maul, C. Hoischen, M. Bienert, General aspects of peptide selectivity towards lipid bilayers and cell membranes studied by variation of the structural parameters of amphipathic helical model peptides, *Biochim. Biophys. Acta* 1558 (2002) 171–186.
- [30] C.J.F. Böttcher, C.M. Van Gent, C. Pries, A rapid and sensitive submicro phosphorus determination, *Anal. Chim. Acta* 24 (1961) 203–204.
- [31] Y.H. Chen, J.T. Yang, H.M. Martinez, Determination of the secondary structures of proteins by circular dichroism and optical rotatory dispersion, *Biochemistry* 11 (1972) 4120–4131.
- [32] M. Dathe, H. Nikolenko, J. Klose, M. Bienert, Cyclization increases the antimicrobial activity and selectivity of arginine- and tryptophan-containing hexapeptides, *Biochemistry* 43 (2004) 9140–9150.
- [33] F.S. Abrams, E. London, Extension of the parallax analysis of membrane penetration depth to the polar region of model membranes: Use of fluorescence quenching by a spin-label attached to the phospholipid polar headgroup, *Biochemistry* 32 (1993) 10826–10831.
- [34] A. Chattopadhyay, E. London, Parallax method for direct measurement of membrane penetration depth utilizing fluorescence quenching by spin-labeled phospholipids, *Biochemistry* 26 (1987) 39–45.
- [35] J. Seelig, Titration calorimetry of lipid–peptide interactions, *Biochim. Biophys. Acta* 1331 (1997) 103–116.
- [36] J. Seelig, S. Nebel, P. Ganz, C. Bruns, Electrostatic and nonpolar peptide–membrane interactions, Lipid binding and functional properties of somatostatin analogues of charge $z=+1$ to $z=+3$, *Biochemistry* 32 (1993) 9714–9721.
- [37] F. Roux, O. Durieu-Trautmann, N. Chaverot, M. Claire, P. Mailly, J.M. Bourre, D.A. Strosberg, P.O. Couraud, Regulation of gamma-glutamyl transpeptidase and alkaline phosphatase activities in immortalized rat brain microvessel endothelial cells, *J. Cell. Physiol.* 159 (1994) 101–113.
- [38] Y. Omid, L. Cambell, J. Barar, D. Connell, S. Akhtar, M. Gumbbleton, Evaluation of the immortalized mouse brain capillary endothelial cell line, b.End3, as an in vitro blood–brain barrier model for drug uptake and transport studies, *Brain Res.* 990 (2003) 95–112.
- [39] D. Eisenberg, Three-dimensional structure of membrane and surface proteins, *Ann. Rev. Biochem.* 53 (1984) 595–623.
- [40] S.C.J. Rall, K.H. Weisgraber, R.W. Mahley, Human apolipoprotein E, The complete amino acid sequence, *J. Biol. Chem.* 257 (1982) 4171–4178.
- [41] B. Bechinger, Membrane insertion and orientation of polyalanine peptides: a $(15)\text{N}$ solid-state NMR spectroscopy investigation, *Biophys. J.* 81 (2001) 2251–2256.
- [42] B. Vogt, P. Ducarme, S. Schinzel, P. Brasseur, B. Bechinger, The topology of lysine-containing amphipathic peptides in bilayers by circular dichroism, solid-state NMR, and molecular modeling, *Biophys. J.* 79 (2000) 2644–2656.
- [43] W.C. Wimley, S.H. White, Designing transmembrane alpha-helices that insert spontaneously, *Biochemistry* 39 (2000) 4432–4442.
- [44] F. Reig, I. Haro, D. Popo, M.A. Egea, M.A. Alsina, Interfacial interaction of hydrophobic peptides with lipid bilayers, *J. Colloid Interface Sci.* 246 (2002) 60–69.
- [45] E.A. Burstein, N.S. Vendenkina, M.N. Ivkova, Fluorescence and the location of tryptophan residues in protein molecules, *Photochem. Photobiol.* 18 (1973) 263–279.
- [46] T.L. Innerarity, R.E. Pitas, R.W. Mahley, Binding of arginine-rich (E) apoprotein after recombination with phospholipid vesicles to the low density lipoprotein receptors of fibroblasts, *J. Biol. Chem.* 254 (1979) 4186–4190.
- [47] S. Keller, I. Sauer, K. Gast, H. Strauss, M. Dathe, M. Bienert, Physicochemical characterization of membrane-mimetic micelles formed by a dipalmitoylated cell-penetrating peptide, *Angew. Chem., Int. Ed. Engl.* 44 (2005) 5252–5255.
- [48] T. Wieprecht, M. Beyermann, J. Seelig, Binding of antibacterial magainin peptides to electrically neutral membranes: thermodynamics and structure, *Biochemistry* 38 (1999) 10377–10387.
- [49] A.S. Ladokhin, P.W. Holloway, Fluorescence of membrane-bound tryptophan octyl ester: a model for studying intrinsic fluorescence of protein–membrane interactions, *Biophys. J.* 69 (1995) 506–517.
- [50] D. Avrahami, Y. Shai, Conjugation of a magainin analogue with lipophilic acids controls hydrophobicity, solution assembly, and cell selectivity, *Biochemistry* 41 (2002) 2254–2263.
- [51] C.T. Pool, T.E. Thompson, Chain length and temperature dependence of the reversible association of model acylated proteins with lipid bilayers, *Biochemistry* 37 (1998) 10246–10255.
- [52] R.M. Peitzsch, S. McLaughlin, Binding of acylated peptides and fatty acids to phospholipid vesicles: pertinence to myristoylated proteins, *Biochemistry* 32 (1993) 10436–10443.
- [53] G. Ponsin, K. Strong, A.M. Gotto Jr., J.T. Sparrow, H.J. Pownall, In vitro binding of synthetic acylated lipid-associating peptides to high-density lipoproteins: Effect of hydrophobicity, *Biochemistry* 23 (1984) 5337–5342.
- [54] F. Eisele, J. Kuhlmann, H. Waldmann, Synthesis and membrane-binding properties of a characteristic lipopeptide from the membrane-anchoring domain of influenza virus A hemagglutinin, *Angew. Chem., Int. Ed. Engl.* 40 (2001) 369–373.
- [55] R. Brasseur, T. Pillot, L. Lins, J. Vandekerckhove, M. Rosseneu, Peptides in membranes: tipping the balance of membrane stability, *Trends Biochem. Sci.* 22 (1997) 167–171.
- [56] J. Ren, S. Lew, Z. Wang, E. London, Transmembrane orientation of hydrophobic alpha-helices is regulated both by the relationship of helix length to bilayer thickness and by the cholesterol concentration, *Biochemistry* 36 (1997) 10213–10220.
- [57] C.A. Dyer, L.K. Curtiss, A synthetic peptide mimic of plasma apolipoprotein E that binds the LDL receptor, *J. Biol. Chem.* 266 (1991) 22803–22806.
- [58] K.H. Weisgraber, Apolipoprotein E: structure–function relationships, *Adv. Protein Chem.* 45 (1994) 249–369.
- [59] T. Kiyota, S. Lee, G. Sugihara, Design and synthesis of amphiphilic alpha-helical model peptides with systematically varied hydrophobic–hydrophilic balance and their interaction with lipid- and bio-membranes, *Biochemistry* 35 (1996) 13196–13204.
- [60] M.A. Clay, G.M. Anantharamaiah, M.J. Mistry, A. Balasubramaniam, J.A. Harmony, Localization of a domain in apolipoprotein E with both cytostatic and cytotoxic activity, *Biochemistry* 34 (1995) 11142–11151.
- [61] M. Tolar, M.A. Marques, J.A. Harmony, Neurotoxicity of the 22 kDa thrombin-cleavage fragment of apolipoprotein E and related synthetic peptides is receptor-mediated, *J. Neurosci.* 17 (1997) 5678–5686.
- [62] D.W. Gaber, S. Handattu, I. Aslan, G. Datta, M. Chaddha, G.M. Anantharamaiah, Effect of an arginine-rich amphipathic helical peptide on plasma cholesterol in dyslipidemic mice, *Atherosclerosis* 168 (2003) 229–237.
- [63] P.W. Park, O. Reizes, M. Bernfield, Cell surface heparan sulfate proteoglycans: selective regulators of ligand–receptor encounters, *J. Biol. Chem.* 275 (2000) 29923–29926.